Atomistic Modeling of Composite Interfaces

M. Deng[a], V.B.C. Tan[a,*], T.E. Tay[a,b] and S.W. Yang[c]

[a]Dept. of Mechanical Engineering, National University of Singapore,
[b]Division of Bioengineering, National University of Singapore,
9 Engineering Drive 1, Singapore 117576
[c]Institute of High Performance Computing, Singapore

ABSTRACT

The performance and strength of many composites, hybrid and thin multi-layered material systems are very much dependent upon the mechanical properties of interfaces. However, the continuum mechanics approach to the characterization of interfacial properties has had limited success because it is often unable to incorporate the effects of molecular and chemical interactions into the model. There is therefore a need to understand and study the influence of these factors on mechanical properties such as adhesion strength at a more fundamental level. In the present work, the interfaces of two common coupling agents and matrix polymers in composites are studied with atomistic modeling and simulation. The polymer matrix is polycarbonate (PC) and the coupling agents studied are gamma amino-propyl-triethoxysilane (AMPTES) and stearic-propyl-triethoxysilane (SPTES). Two interface models, SPTES/PC and AMPTES/PC were built and the work of adhesion was calculated from molecular dynamics (MD) simulation. The separation of the coupling-agents/matrix interfaces was simulated using MD calculations and the mechanical properties were obtained. It is shown that the higher work of adhesion of the interface is not equal to higher interfacial toughness.

1. INTRODUCTION

The determination and characterization of the mechanical properties of material interfaces has always been an area of interest because the integrity of material interfaces plays a key role in the robustness of devices and material systems. However, the understanding of interfacial properties continually poses a challenge because material interfaces are usually of the nanometer length scale. At this scale, continuum mechanics break down and techniques for sub-micron experiments are still not fully developed. For instance, some researchers believe interfacial strength is best described as adhesion [1, 2], while others believe that the strength of interfaces is better described by the energy required to separate the constituents [3, 4]. Theoretical analyses based on continuum mechanics approach and experimental investigation have seen limited success because the effects of molecular and chemical interactions at material interfaces are not accounted for in many analytical models and are difficult to ascertain experimentally [5,6]. Molecular dynamics (MD) simulation can show detailed molecular motions in interfaces and has become increasingly popular because of significant improvements in computer speed. MD simulations can provide information on interfacial strength and mechanical properties of the interfacial constituents at a more fundamental level.

Central to all MD calculations is the selection of an appropriate force field to describe the potential energy surface. The potential controls the motions of the polymer chains because forces for molecular motion are derived from the first spatial derivatives of the potential. In general, the force fields of polymer systems are derived from the sum of bond, crossterm and nonbond interactions. Force fields are classified into two groups [7]. The classical force fields (Class I), like MM2 [8], AMBER [9] and CHARMm [10,11], etc, consider only harmonic bond and nonbond terms, reflecting electrostatic and van der Waals interactions etc. To improve on modeling accuracy, Class II force fields, such as CFF [12,13], which was designed specially for alkane molecules, and MM3 [14], were carried out for macromolecules by including anharmonic

bond and cross terms. They can therefore be used directly for isolated molecules, condensed phases, and macromolecular systems without modification [7].

This paper focuses on using MD simulation to study the mechanical strength of polymer-polymer interfaces involving sizing agents. This is of interest in fiber-reinforced composites where debonding at the fiber-matrix is of great concern but yet not well understood. While there have been reports of MD simulations of polymer-polymer interfaces [17-24], very little is reported on MD simulations in determining the mechanical strength of such material systems. One reason for the lack of literature is the prohibitively large numbers of molecules that need to be included in the model in order to relate to practical applications. With the huge computational task of force-field calculation, high-performance computer resource becomes necessary. Another reason is that, unlike the crystal lattice models of metals which have regular atomistic arrangements, the methodology for building the initial conformation of polymers is not well established. In fact, the construction of a "reasonable" amorphous packing of polymer bulk for the initial structure is by itself an active area of research [25-30].

Very often the amorphous conformation is obtained by relaxing an initial "guess" structure through energy minimization or simulated annealing with incremental changes in temperature and/or pressure [29] until the final state is achieved. The Amorphous Cell model [25] is commonly used to create initial structures and has been used as the starting point for many MD simulations in the study of polymers and polymer interfaces [17-24].

Reiter et al [17] studied interfaces between polymer melts through MD simulation and found that thicker and more stable interfaces than predicted by theory can be obtained with antiperiodic boundary conditions. Similar studies on the interfacial thickness and interactions of several kinds of polymers obtained from MD simulations have also been reported by Yao et al [19]. Mansfield and Theodorou [18] proposed a method to predict the internal energy contribution to the adhesion of materials. A short review of the development of MD simulation for predicting bulk and interfacial properties of organic coatings can be found in a report by Yarovsky [20], in which another method was used to study the interfacial stability, degree of curing in polymers and permeability to small molecules. The same methodology was applied to investigate a system of an inorganic substrate with a layer of cured epoxy coating [21]. The study reported on the barrier properties and shrinkage of the resin. A similar method was also developed independently by Natarajan et al [22] and Clancy and Mattice [23] to study the interfacial region and the work of adhesion of Polypropylene (PP)-PP, PP-Poly(1,4-cis-butadiene) (PBD), PBD-PBD [22], and polyolefin interfaces [23]. Okada et al [24] used the same method to study the interfacial properties and the separation of a large amorphous poly(methyl methacrylate) (PMMA)-poly(tetrafluoroethylene) (PTFE) system using non-equilibrium MD calculation [24, 31]. Despite the interest in material interfaces, the mechanical properties of polymer-polymer interfaces, specifically, the fiber-matrix interfaces of fiber-reinforced composites, by MD simulation have not yet to be reported.

In the present study, the interfaces of a matrix and coupling agents are modeled. The matrix used is polycarbonate (PC) and the coupling agents studied are gamma amino-propyl-triethoxysilane (AMPTES) and stearic-propyl-triethoxysilane (SPTES). Two atmostic models of SPTES-PC and AMPTES-PC interfaces were constructed and an algorithm is proposed to investigate the mechanical properties of polymer interfaces. Special effort was made to use the smallest possible degrees of freedom as the MD simulation was carried out on desktop PCs.

2. MOLECULAR MODELING OF THE INTERFACES

2.1 Molecular models

Figure 1 shows a fiber embedded in matrix, as typically found in fiber-reinforced composites.

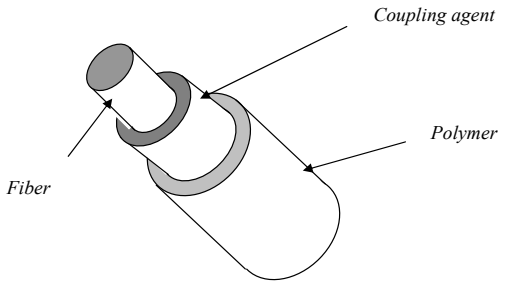

Fig. 1. Model of fiber/matrix interfaces.

The interface presented comprises a glass fiber and PC matrix with a coupling agent - AMPTES or SPTES. The structures of PC, AMPTES and SPTES are shown in Fig.2.

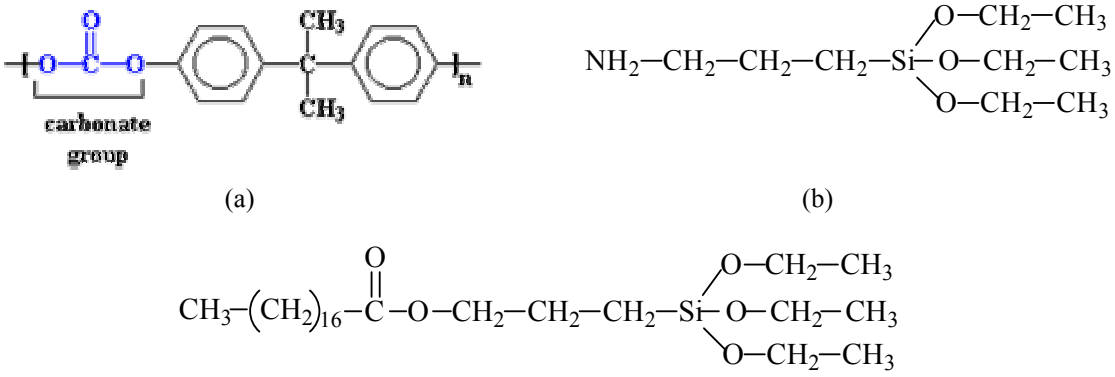

Fig.2. Structures of the matrix and silanes. (a) Polycarbonate (PC) monomer. (b) Gamma amino-propyl-triethoxysilane (AMPTES) (c) stearic-propyl-triethoxysilane (SPTES)

In the fabrication of fiber-reinforced composites, the fiber is first cured with some coupling agents. The reactions give rise to a crosslinking process, which in the present case (glass fiber cured by silanes) is

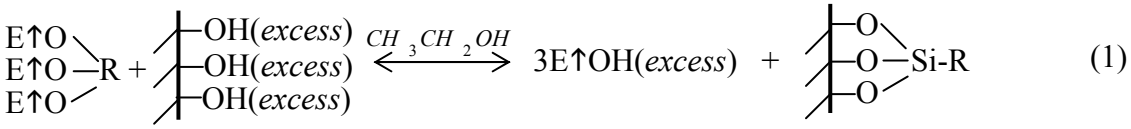

(1)

Here, R- is *stearic-propyl-* or *amino-propyl-* and E is $-CH_2CH_3$ in the present models.
Figure 3 shows the molecular structure at the glass-PC interface together with AMPTES after the crosslinking reaction given in eq. 1. Due to the strong –Si–O–Si– bonds between the glass fiber and silanes, the "weakest site" of the composite interfaces would be at either the interface of the silane-matrix or inside the bulk of silanes and/or matrix (Fig.3). Hence, it is sufficient to model just the PC and silane and the interfaces between them to study the mechanical properties of fiber-matrix interfaces.

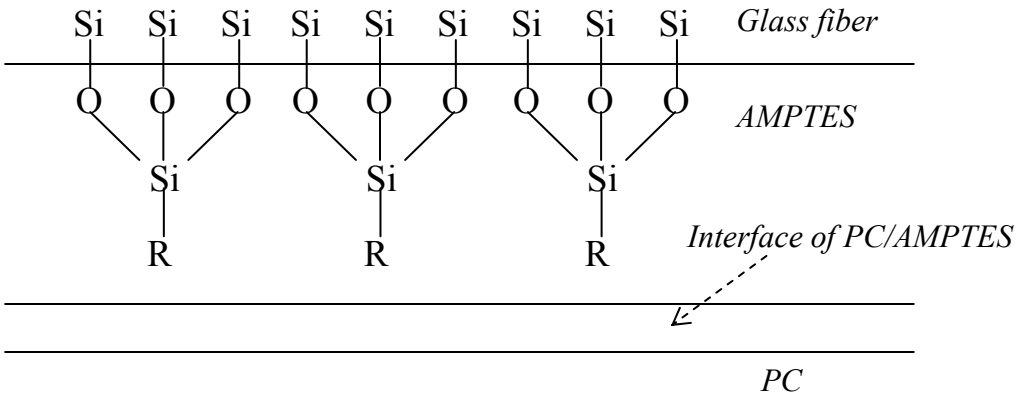

Fig.3. Molecular structures of glass-PC interface with AMPTES present.

All the MD calculations were performed using a commercial software - Material Studio (*Accelrys Inc.*). In the MD calculations, COMPASS, a Class II force field [15, 16], was chosen for the MD calculation because it was developed from CFF [12, 13] to accommodate most organic molecules, including silanes and rings.

2.2 Molecular Modeling of Polymer Interfaces

The Amorphous Cell [25, 32] procedure was used to build atomistic models of the PC and silane bulk systems. The main cells have one main chain with 17 monomers for PC, 16 molecules for AMPTES and seven molecules for SPTES. To obtain a statistical average, five amorphous cell samples of each material were built. The bulk densities [33] and cell constants of the amorphous cells are listed in Tab. 1.

"Table 1. Cell properties of bulk materials using Amorphous cell model"

	PC	AMPTES	SPTES
Density (kg/cm^3)	1.20	0.95	0.95
Cell constants(Å)	18.16	18.36	18.66

The energies of the cells are first minimized using the conjugate gradient method with a convergence criterion of RMS atomic force cutoff of 0.1 kcal/mol·Å. The molecules in each amorphous cell are set to vibrate by NVT molecular dynamics for 50ps at 300K [22]. The configuration with the minimum potential energy is then selected and minimized to a convergence of 0.01 kcal/mol·Å, with the conjugate gradient method.

The thin surface films of PC and silanes are constructed from the amorphous cells by extending the periodic box of the cells in the z-direction to about 60 Å and then padding the end of the box with a vacuum of about 50 Å length. This prevents the parent chains from interacting with their images along *z* direction while keeping the cell size small enough to remain computationally tractable [35, 36].

In the simulations, the equations of motion were integrated with the velocity version of the Verlet algorithm [34] at 300K with a time step of 1.0fs. A cutoff distance of 8.5 Å (based on neutral groups of atoms) was used for the nonbonded interactions.

The thin films are subjected to molecular energy minimization followed by 50 ps of NVT MD simulation at about 300K. To excite the thin films, the cells are heated to about 600K for 100 ps followed by 100 ps MD at about 300K. The snapshots with lowest potential energy were chosen to construct the final surface thin film conformations through energy minimizations to a convergence of 0.1 kcal/mol·Å with the conjugate gradient method. The surface energies, γ, of the PC and silanes are obtained from the energy difference between the thin film cells and corresponding bulk amorphous cells divided by the surface areas created [23]:

$$\gamma = \frac{E_{film} - E_{bulk}}{2A} \qquad (2)$$

Here, A is the area of each of the two surfaces of the thin films, and E_{film} and E_{bulk} are the energies of the thin film cells and bulk material cells.
Material interfaces cells were created by putting two thin films together with the surfaces in contact without overlapping [20]. The potential energy of the contacting films was minimized followed by 100ps of MD simulations at about 300K. The cells are then heated at about 600K for 100ps to facilitate the diffusion of the two materials across the interface. This is followed by 100ps of NVT MD calculations at 300K to simulate annealing. The snapshots with lowest potential energy were chosen and subjected to energy minimization again to a convergence of 0.1 kcal/mol·Å with the conjugate gradient method to obtain the final interface conformations. Two material interfaces, PC-AMPTES (Fig.4) and PC-SPTES, were constructed in this manner for this paper.

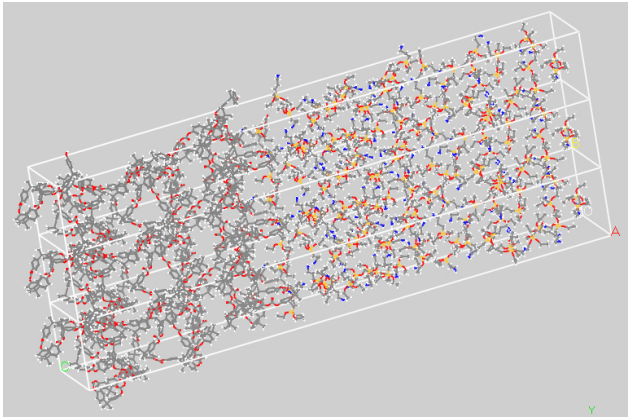

Fig.4. PC/AMPTES interface. (left: PC, right: AMPTES)

2.3 Work of adhesion and mechanical properties of interfaces
The work of adhesion W_{AB} per unit area is obtained from the difference in energy between the interfacial system and the energy of the two individual thin films which were used to build the interface.

$$W_{AB} = (E_{film\ A} + E_{film\ B} - E_{interface})/2\mathrm{A} \qquad (3)$$

The interfacial tension γ_{AB}, is then obtained from the Dupre equation [37],

$$\gamma_{AB} = \gamma_A + \gamma_B - W_{AB} \quad (4)$$

where the free surface energies γ_A and γ_B are obtained from equation (2).
The mechanical properties of the interfaces were studied by prescribing an axial extension on the interface cells in the z-direction (i.e. thickness direction). The incremental strain applied to the periodic cells at each step of the simulation was,

$$d\varepsilon_z = \begin{bmatrix} -1 & 0 & 0 \\ 0 & -1 & 0 \\ 0 & 0 & 2 \end{bmatrix} \times 10^{-3} \quad (5)$$

This same strain increment was also used by Mott et al [38] to study the plastic deformation of bulk polypropylene cells. They used energy minimization through conjugate gradient minimization which does not allow for temperature effects to be included. In the present article, the strain increment was applied perpendicularly to the interface with 1ps NVT MD equilibration at 300K for each increment. The force and displacement histories were recorded to obtain the stress-strain curves at room temperature. With this approach, it is possible to investigate the polymer interface at any temperature and thus attach more practical applications to the simulation. In the MD calculations, the non-bond energy cutoff used is 5.5 Å. For an interface cell of 55 residues with 3687 atoms, it took an IBM PC, with a 2.3GHz Pentium 4 CPU, 75 minutes for 1000 steps of simulation.

3. Results and discussion

3.1 Bulk properties of amorphous cells

Figure 4 shows the interface cell of PC-AMPTES and Table 2 shows the work of adhesion calculations of the two interfacial systems using eq. 2~3.

"Table 2. Energy components (kJ/mol) of PC-silane interface cells, and their contribution to work of adhesion (mJ/m^2)."

	PC/AMPTES interface		PC/SPTES interface	
	$E_{interface}$	W_{AB}	$E_{interface}$	W_{AB}
Total Potential Energy	-5285.94	98.11	-3897.80	106.39
Restraint	-165.49	51.31	-139.13	-39.54
Bond stretching	259.98	-1.96	271.16	0.05
Bond angle bending	563	-17.00	681.60	11.62
Torsion	-2206.37	4.88	-2248.10	42.81
Cross terms	-458.59	3.14	-479.29	0.68
Nonbond	-3284.86	57.89	-1992.15	89.67

The energy of the PC-AMPTES and PC-SPTES interfaces are listed in the second and fourth columns of Tab. 2 and the work of adhesion are listed in the third and fifth columns, respectively. Each component of the energy contributions is also listed.

"Table 3. Summary of surface tension, work of adhesion (erg cm^{-2}) and interfacial tensions(erg cm^{-2}) of PC(γ_A)-silane(γ_B) interfaces."

Interfaces	γ_A	γ_B	W_{AB}	γ_{AB}
PC/AMPTES	42.44	18.08	98.11	-37.59
PC/SPTES	42.44	19.25	106.39	-44.70

Table 3 is a summary of the surface tension γ_A and γ_B, work of adhesion W_{AB} and interfacial tension γ_{AB} for the two PC-silane interfaces calculated from equations 2, 3 and 4 respectively. The surface tension predicted for PC is very close to the reported value of 45 mJ/m^2 [40]. It also shows that SPTES has higher surface tension than AMPTES. The table shows that the work of adhesion for PC-SPTES is higher than the work of adhesion for PC-AMPTES. This is expected because SPTES has a higher surface tension than that of AMPTES.

3.2 Mechanical properties of the interfaces

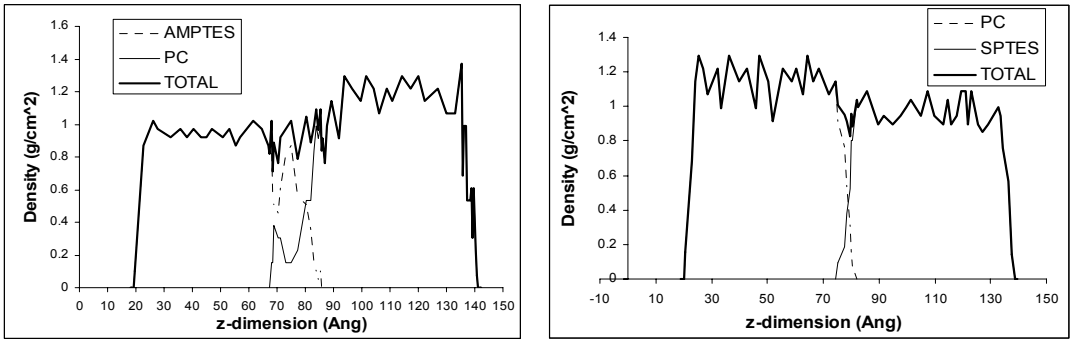

(a) (b)

Fig.5. Density profile of PC-silane interfaces: (a) PC-AMPTES before tensile deformation, (b) PC-SPTES before tensile deformation, (c) PC-AMPTES at 53% tensile strain, (d) PC-SPTES at 53% tensile strain.

Figure 5 shows the density profiles of the interfaces of PC-AMPTES and PC-SPTES. The density is plotted as a function of position in the thickness direction (i.e. along the z-coordinate) on the central axial mass of the interfacial cell. From the depth of diffusion of the chains of the two constituents, the thickness of the PC-AMPTES and PC-SPTES interfaces can be determined to be about 18 Å and 8 Å, respectively. These values are of the same order of magnitude as other reported values of immiscible polymer-polymer interfaces thickness - 10~15 Å for PP-PBD [22], 15~20 Å for PP-PP [23], 15~25 Å for PS-PMMA [41] and 22~38 Å for PS-PE [42], and 20 Å for PMMA-PTFE [24]. It should be noted that the thickness of the PC-AMPTES interface is twice as large as that of the PC-SPTES interface even though they were formed under the same heating and annealing process and both silanes have similar free surface energies as shown in Table 3.
To study the mechanical properties of the silane-PC interfaces, the two interface cells are pulled apart by imposing incremental strains in the thickness direction according to equation 5. For each strain increment, 1000 steps of NVT MD equilibrium at 300K with a time step of 1.0fs are performed. The component of stress in the thickness direction plotted against the strain of the cell is shown in Fig.6.

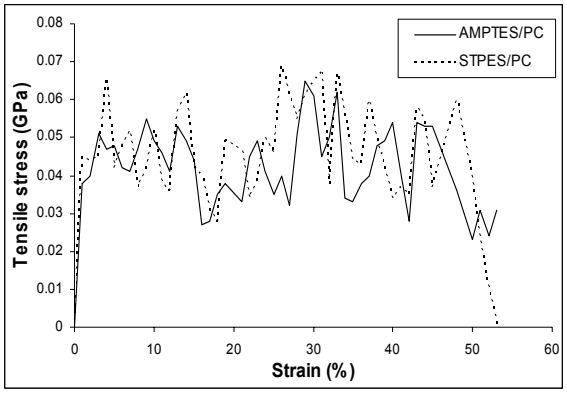

Fig.6. Stress-Strain curve of Silane-PC interfaces under tensile loading.

From the stress-strain curves, the elastic-plastic properties of the interface cells can be deduced. It is interesting to note that at 53% strain, the PC-AMPTES interface can still continue to sustain tensile loads whereas the interaction in the interfacial cell of PC-SPTES has reduced significantly and is no longer able to sustain any tensile stress beyond 53% strain. This is despite the fact that the work of adhesion of PC-SPTES is larger than that of PC-AMPTES (Tab.2). The results can be explained by that the deeper diffusion of PC chains inside the surface of AMPTES resulted in improved ductility and enabled the AMPTES/PC interface to sustain higher strains than the SPTES/PC interface. The results can also be deduced from the equation of diffusion coefficient,

$$D_M = N_e \frac{\phi^2(1-\phi)^2}{z'}\left[\frac{1}{N_A\phi} + \frac{1}{N_B(1-\phi)}\right]^2 \qquad (6)$$

where D_M is the diffusion coefficient, Ne ~ 200, ϕ is volume fraction of the interface, z' is a frictional coefficient, N_A and N_B are number of monomers of the two polymer chains. From the equation, it is shown that the interdiffusion of polymer-polymer interfaces is mainly controlled by the fast (short) chains and less dependent on the slow (long) chains [43]. Similar observations were reported by Zhang Newby et al [44] in which it was concluded that higher surface tension does not necessarily imply higher adhesion.

4. CONCLUSIONS

The mechanical properties of PC-AMPTES and PC-SPTES composite interfaces were investigated through atomistic simulation using a combination of conjugate gradient energy minimization and molecular dynamics. AMPTES and SPTES are coupling agents commonly used at the fiber-matrix interfaces of fiber-reinforced composites. The surface energies of PC, AMPTES and SPTES were obtained from atomistic simulations by considering the difference in the potential energies of amorphous cells of bulk materials and amorphous cells of materials with a free surface. The work of adhesion of the interfaces of PC-AMPTES and PC-SPTES were also determined by considering the energies of PC, AMPTES and SPTES individually and the energies of PC-AMPTES and PC-AMPTES systems. It was found that SPTES has a higher surface energy than AMPTES and, similarly, the work of adhesion of PC-SPTES was also found to be higher than PC-AMPTES. However, in MD simulations of PC-SPTES and PC-AMPTES

systems under tension perpendicular to the interface, both systems were found to have similar flow stress but the PC-SPTES system was found to separate at a much lower strain than the PC-AMPTES system. Hence, the work of adhesion may not necessarily be an indication of the toughness of bi-material systems under mechanical loading.

ACKNOWLEDGEMENTS

This is dummy text. It has nothing to say whatsoever. It is only placed here for display purposes. You can continue reading this text if you wish but you will learn nothing.

Reference:

1. **Di Landro, L.** and **Pegoraro, M.**, "Evaluation of residual stresses and adhesion in polymer composites", *Composites A*, **27**/9 (1996), 847-853.
2. **Drzal, L.T., Sugiura, N.** and **Hook, D.**, "The role of chemical bonding and surface topography in adhesion between carbon fibers and epoxy matrices", *Compos Interface.*, **4** (1997), 337-354.
3. **Wu, H.F.** and **Claypool, C.M.**, "An analytical approach of the microbond test method used in characterizing the fibre-matrix interface", *J Mater Sci Lett.*, **10** (1991), 260-262.
4. **Beckert, W.** and **Lauke, B.**, "Critical discussion of the pull-out test", *Compos Sci Technol.*, **57**/12, (1997), 1689-1706.
5. **Pisanova, E., Zhandarov, S.** and **Mader, E.**, "How can adhesion be determined from micromechanical test?", *Composites A*, **32**, (2001), 425-434.
6. **Nairn, J.A., Liu, Y.C.** and **Galiotis, C.**, "Analysis of stress transfer from the matrix to the fiber through and imperfect interface: application to Raman data and the single-fiber fragmentation test", *Fiber, matrix, and interface properties, ASTM STP 1290, Philadelphia: American Society for Testing and Materials*, (eds.Spragg CJ and Drzal LT), (1996), 47-66.
7. **Hwang, M.J., Stockfisch, T.P.** and **Hagler, A.T.**, "Derivation of Class II Force Field. 2. Derivation and Characterization of a Class II Force Field, CFF93, for the Alkyl Functional Group and Alkane Molecules", *J Am Chem Soc.*, **116** (1994), 2515-2525.
8. **Allinger, N.L.**, "Conformational Analysis 130. MM2. A Hydrocarbon Force Field Utilizing V_1 and V_2 Torsional Terms", *J Am Chem Soc.*, **99** (1977), 8127-8134.
9. **Weiner, S.J., Kollman, P.A., Case, D.A., Singh, U.C., Chio, C., Alagona, G., Profeta, Jr S.** and **Weiner, P.**, "A New Force Field for Molecular Mechanical Simulation of Nucleic Acids and Proteins", *J Am Chem Soc.*, **106** (1984), 765-784.
10. **Brooks, B.R., Bruccoleri, R.E., Olafson, B.D., States, D.J., Swaminathan, S.** and **Karplus, M.**, "CHARMM: A Program for Macromolecular Energy, Minimization, and Dynamics Calculations", *J Comput Chem.*, **4** (1983), 187-217.
11. **Smith, J.C. and Karplus, M.**, "Empirical Force Field Study of Geometries and Conformational Transitions of Some Organic Molecules", *J Am Chem Soc.*, **114** (1992), 801-812.
12. **Maple, J.R., Dinur, U.** and **Hagler, A.T.**, "Derivation of Force Fields for Molecular Mechanics and Dynamics from ab initio Energy Surfaces", *P Natl Acad Sci USA.*, **85**/15 (1988), 5350-5354.
13. **Maple, J.R., Hwang, M.J., Stockfisch, T.P., Dinur, U., Waldman, M., Ewig, C.S.** and **Hagler, A.T.**, "Derivation Of Class II Force Fields .1. Methodology and Quantum Force Field for the Alkyl Functional Group and Alkane Molecules", *J Comput Chem.*, **15**/2 (1994), 162-182.
14. **Allinger, N.L., Yuh, Y.H.** and **Lii, J-H**, "Molecular Mechanics, The MM3 Force Field for Hydrocarbons", *J Am Chem Soc.*, 111 (1989), 8551-8575.
15. **Sun, H.** and **Rigby, D.**, "Polysiloxanes: Ab Initio Force Field And Structural, Conformational And Thermophysical Properties", *Spectrochim Acta A.*, **53** (1997), 1301-1323.
16. **Sun, H.**, "COMPASS: An ab Initio Force-Field Optimized for Condensed-Phase Applications - Overview with Details on Alkane and Benzene Compounds", *J Phys Chem-US*, **102**/38 (1998), 7338-7364.
17. **Riter J., Zifferer G.** and **Olaj, O.F.**, "Monte Carlo Studies of the Interface between Two Polymer Melts", *Macromolecules*, **23** (1990), 224-228.
18. **Mansfield, K.F.** and **Theodorou, D.N.**, "Atomistic Simulation of a Glassy Polymer/ Graphite Interface", *Macromolecules*, **24** (1991), 4295-4309.

19. **Yao, S., Kamei, E.** and **Matsumoto, T.**, "The chemical structure dependence of interaction strength between polymers and mobility of polymer chains in the polymer interface", *Comput Theor Polym S.*, **7** (1997), 25-33.
20. **Yarovsky, I.**, "Atomistic Simulation of Interfaces in Materials: Theory and Applications", *Aust J phys.*, **50** (1997), 407-424.
21. **Yarovsky, I.** and **Evans, E.**, "Computer Simulation of Structure and Properties of Crosslinked Polymers: application to epoxy resins", *Polymer*, **43** (2002), 963-969.
22. **Natarajan, U., Misra, S.** and **Mattice, W.L.**, "Atomistic Simulation of a Polymer-polymer Interface: interfacial energy and work of adhesion", *Comput Theor Polym S.*, **8** (1998), 323-329.
23. **Clancy, T.C.** and **Mattice, W.L.**, "Computer Simulation of Polyolefin Interfaces", *Comput Theor Polym S.*, **9** (1999), 261-271.
24. **Okada, O., Oka, K., Kuwajima, S.**, **Toyoda, S.** and **Tanabe, K.**, "Molecular Simulation of an Amorphous Poly (methyl methacrylate) – Poly (tetrafluoroethylene) interface", *Comput Theor Polym S.*, **10** (2000), 371-381.
25. **Theodorou, D.N.** and **Suter, U.W.**, "Detailed Molecular Structure of a Vinyl Polymer Glass", *Macromolecules*, 18 (1985), 1467-1478.
26. **Brostow, W.** and **Kubat, J.**, "Molecular-dynamics simulation of stress relaxation on a triangular lattice", *Phys Rev B.*, **47** (1993), 7659–7667.
27. **Gusev, A.A., Zehnder, M.M.** and **Suter, U.W., "**Elasticity of solid polymers as a result of thermal motions", *Macromolecules*, **27** (1994), 615-616.
28. **Kotelyanskii, M., Wagner, N.J.** and **Paulatis, M.E.**, "Building Large Amorphous Polymer Structures: Atomistic Simulation of Glassy Polystyrene", *Macromolecules*, **29**/26 (1996), 8497-8506.
29. **Muller, M., Nievergelt, J., Santos, S.** and **Suter, U.W.**, "A Novel Geometric Embedding Algorithm for Efficiently Generating Dense Polymer Structures", *J Chem Phys.*, **114**/22 (2001), 9764-9771.
30. **Santos, S., Suter, U.W., Muller, M.** and **Nievergelt, J.**, "A Novel Parallel-rotation Algorithm for Atomistic Monte Carlo Simulation of Dense Polymer Systems", *J Chem Phys.*, **114**/22 (2001), 9772-9779.
31. **Gao, J.** and **Weiner, J.H.**, "Simulated Polymer melt stress relaxation. I. plateau behavior", *J Chem Phys.*, **103**/4 (1995), 1614-1620.
32. *Polymer User Guide*, Accelrys Inc., San Diego, USA. 1996.
33. **Mark, J.E.** (ed.), *Physical Properties of Polymers Handbook*. Woodbury, New York, 1996.
34. **Allen, M.P.**, and **Tildesley, D.J.**, *Computer Simulation of Liquids*. Clarendon Press, Oxford, 1987.
35. **Mansfield, K.F.** and **Theodorou, D.N.**, "Atomistic Simulation of a Glassy Polymer Surface", *Macromolecules*, **23** (1990), 4430-4445.
36. **Misra, S., Fleming, P.D.** and **Mattice, W.L.**, "Structure and energy of thin films of poly-(1,4-cis-butadiene): a new atomistic approach", *J Comput-aided Mater.*, **2** (1995), 193-205.
37. **Lee, L.H.**, "The Chemistry and Physics of Solid Adhesion", *Fundamentals of Adhesion*, (ed. Lee LH), **1** (1991), Plenum Press, New York.
38. **Mott, P.H., Argon, A.S.** and **Suter, U.W.**, "Atomistic modeling of plastic deformation of glassy polymers", *Philos Mag A.*, **67**/4 (1993), 931-978.
39. **Theodorou, D.N.** and **Suter, U.W.**, "Atomistic Modeling of Mechanical Properties of Polymeric Glasses", *Macromolecules*, **19** (1986), 139-154. "Local Stucture and the Mechanism of Response to Elastic Deformation in a Glassy Polymer", *Macromolecules*, 19 (1986), 379-387.
40. **Brandup, J., Immergut, E.H.** and **Grulke, E.,** *Polymer Handbook*, 4th edition, John Wiley, New York, 1999.
41. **Fernandez, M.L., Higgins, J.S., Penfold, J., Ward, R.C., Shackleton, C.** and **Walsh, D.J.**, "Neutron reflection investigation of the interface between an immiscible polymer pair", *Polymer*, **29**/11 (1988), 1923-1928.
42. **Hermes, H.E., Higgins, J.S.** and **Bucknall, D.G.**, "Investigation of the melt interface between polyethylene and polystyrene using neutron reflectivity", *Polymer*, **38**/4 (1997), 985-989.
43. **Brochard-Wyart, F.**, Kinetics of Polymer-Polymer interdiffusion, *Fundamentals of Adhesion*, (ed. Lee L-H), 181-206, Plenum Press, New York, 1991.
44. **Zhang Newby B, Chaudhury MK** and **Brown HR**, "Macroscopic Evidence of the Effect of Interfacial Slippage on Adhesion", *Science*, **269** (1995), 1407-1409.